Advances in Hydrogen Energy Technologies:
Oportunities and Challenges in a Hydrogen Economy
4th International Seminar - November 10-11, 2011, Viana do Castelo - Portugal

MEA degradation in PEM Fuel Cell: a joint SEM and TEM study

R.A. Silva[1], T. Hashimoto[2], G.E. Thompson[2] and C.M. Rangel[1]

[1]LNEG, Fuel Cells and Hydrogen Unit, Paço do Lumiar,22 1649-038 Lisboa, Portugal
email: raquel.silva@lneg.pt; carmen.rangel@lneg.pt
[2]The University of Manchester, Corrosion and Protection Centre, Manchester M13 9PL, UK
email: george.thompson@manchester.ac.uk

Abstract

One of the important factors determining the lifetime of polymer electrolyte membrane fuel cells (PEMFCs) is membrane electrode assembly (MEA) degradation and failure. The lack of effective mitigation methods is largely due to the currently very limited understanding of the underlying mechanisms for mechanical and chemical degradations of fuel cell MEAs.
This work reports on the effect of 1500 h operation of an eight-cell stack Portuguese prototype low power fuel cell. A performance decrease of 34%, in terms of maximum power, was found at the end of testing period.
A post-mortem analysis by SEM and TEM was done for most cells of the fuel cell. Loss of the PTFE ionomer in the anode and cathode catalytic layers; morphological changes in the catalyst surfaces such as loss of porosity and platinum aggregation, deformation on the MEA components (anode, cathode and membrane) were identified. Others, like delamination and cracking were also detected. Catalyst migration and agglomeration on the interface of the electrodes was observed at cells 2, 4, 6 and 7. A platinum band was also detected on the membrane at 2 μm apart from the anode of cell 4. In some cases, dissolution occurred with re-deposition of the platinum particles with faceted shape; in other cases, migration and agglomeration occurred with the original spherical shape maintained.

Keywords: *PEM fuel cell, MEA degradation, SEM, TEM.*

1 Introduction

A growing interest in the research on performance degradation of PEM fuel cells is evident in the current literature associated to the need of developing durable PEM fuel cells that can be made part of practical applications [1–8]. Lifetime, reliability and cost are still issues affecting the commercialization of proton exchange membrane (PEM) fuel cell systems.

It is known that PEM fuel cells will gradually degrade in performance due to materials deterioration, but operation conditions and poor water and/or heat management are also included in the possible causes for degradation[9].

Many researchers [10-13] have indeed observed microstructure changes when comparing aging membrane electrode assemblies (MEAs) with fresh ones. These changes or failures in MEAs result in a gradual reduction of ionic conductivity, an increase in total cell resistance, a reduction of active sites, a reduction of voltage, and a loss of output power [11]. As crucial parts of MEAs, catalyst layers (CLs) are examined post-mortem through transmission electron microscopy (TEM) and scanning electron microscopy (SEM). The main CLs microstructural changes that had been observed are: cracking, delamination, loss of carbon-supported catalyst clusters, dissolution of the electrolyte (Nafion ionomer), catalyst particle migration, catalyst dissolution and re-deposition.
These phenomena are relatively common, especially under dynamic operating conditions. So the microstructure, especially in CLs, is arguably a critical point for improving the durability of PEMFCs and more and more researchers are focusing on elucidating the mechanism of microstructure changes in CLs and their effects on performance[10-13].

The emphasis of this work is in the post-mortem analysis of an eight-cell stack and in the determination of degradation modes using a joint SEM and TEM analysis.

2 Experimental

An eight-cell stack with own designed flow field graphite plates, integrated in a series configuration was used in this work. The open cathode allows feeding with air, which is designed to contribute to water removal and stack cooling. An air fan located at the edge of the cathode manifolds was used to provide an excess air stoichiometry condition. The cells were fitted with a commercial MEA which uses Nafion 111.
The stack was previously activated by a series of potentiodynamic and potentiostatic cycles before use [14]. Polarization curves were conducted, using an own purpose built PEM test station. Operating conditions used were optimized in previous work [15].
The stack was subject to 12 experimental cycles after the activation procedure, corresponding to total operation time of 1500h. A typical cycle is represented on figure 1.

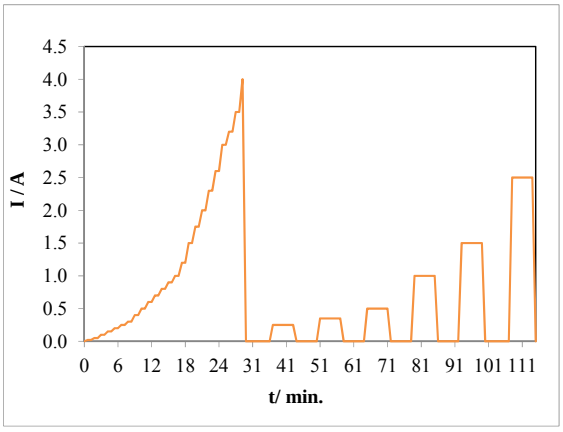

Fig. 1. A typical cycle to which the fuel cell was submitted, after the activation procedure.

After a performance decrease of 34 % regarding the maximum power the stack was dismantled for microstructural analysis. The aged MEAs cycled from the above described procedure were examined by Transmission Electron Microscopy (TEM) and Scanning Electron Microscopy (SEM).
Cross sections of the MEAs samples were observed for morphological and elemental composition changes using a Philips scanning electron microscope, Model XL 30 FEG, coupled to an energy dispersive spectrometer, EDS, allowing elemental mapping. SEM observation was conducted to study the morphological changes of the MEA, including thickness variations, cracking, delamination, platinum clustering and other changes which may decrease the stack voltage at a given demanded current, thus affecting performance.
TEM of individual cells of the studied stack was undertaken using a Tecnai F30 field emission gun instrument operated at an accelerating voltage of 300 kV. Cross sections were prepared by ultramicrotomy using a Leica Ultracut UCT apparatus. Elemental analysis was performed with an Energy Dispersive X-Ray spectroscopy system attached to the microscope.

3 Results

Joint analysis of SEM and TEM results allowed detailed information on micro and macro structures, as well as the chemical composition of the materials and components after a reduction in performance of 34 %, regarding maximum power, in the fuel cell under study.
This information is vital for the continued development of all the components constituting a fuel cell stack and for understanding how these components interact and change under different operating conditions. This information is used when predicting and optimizing stack performance and lifetime.

3.1 Scanning electron microscopy

SEM is a common tool for morphology analysis of catalytic layers which delivers high resolution surface images with a wide range of magnifications. Some important defects were observed when this technique was used.
Typical results can be observed in Figure 2 for the anodic layer for cells 2, 4 and 7 which appear markedly different from the unused sample. Images were taken at 25000 X magnification.
Surface area seems to be lost with cycling. After use and for all the cells, the catalytic layers present a more compact and less porous structure when compared with the unused layers. Part of the problem is probably resulting from the clamping forces to which the cells of the stack are subjected in the sealing and assembly process. Compressing the cathode might have contributed to alter the original morphology. This was more evident for cell 8 for which it was not possible to peeled away the carbon paper.
Another observation of the CLs using SEM, was the gas diffusion layer (GDL) debris. After fuel cell dismantling process all the cells showed, on both anode and cathode, GDL residues that remains attached to the CLs.

Figure 3 shows the GDL debris for cell 2 and cell 7. In the last cell of the stack, it was not possible to remove the GDL at the anode and it was very difficult to remove it at the cathode, leaving carbon fibers from GDL attached to the catalyst surface.

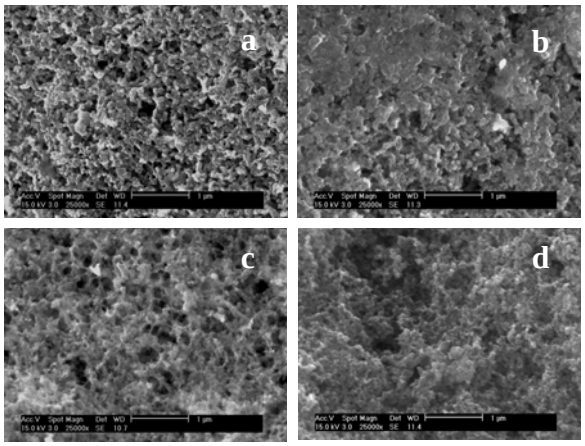

Fig. 2 SEM anode surface morphology for cells 2 (a); 4 (b), 7 (c) and unused sample (d).

This observation corroborates the idea that a high assembly pressure was used in the assembly of the stack and caused the bipolar plate to press the GDL into the catalyst layer. Whilst not the purpose of this study, it is considered important to find, in the future, an optimal torque for this stack design and for the materials used on its construction, establishing a compromise between the tightness of the stack, the contact resistance and the deformation of the different materials.

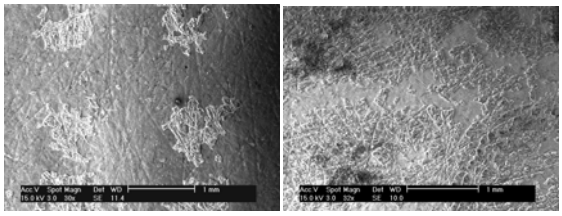

(a) (b)

Fig. 3 GDL debris at anodic layers of cell 2 (a) and Cell 7 (b), after 1500 h of operation.

Determination of MEA components thickness was also carried out with SEM, on MEAs cross-sections.

Figure 4 shows for three MEA components (membrane, anodic and cathodic CLs) their thickness variation comparatively to the unused MEA. The cathode thinning occurs in all the cells being more evident for the cell that suffered the highest degree of degradation and for which the assembling pressure have more drastic consequences (Cell 8). The thickness variations have an effect on the resistance through the MEAs. The thinner areas of the catalyst layer will have a lower electronic resistance, while the thinner electrolyte areas lower ionic resistance.

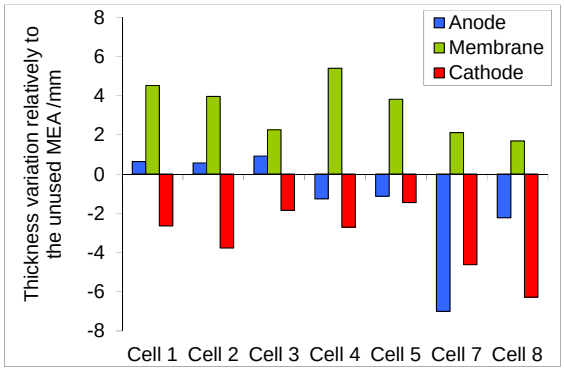

Fig. 4 Thickness variation of MEA components for some of the stack cells, relatively to the unused MEA.

The cathode of all cells showed a thinning which is more pronounced as the cells were farther to the hydrogen inlet in the stack. Cell 8 showed a thinning of about 47% after all the tests. At the anodic layer the thinning is significant only for cells 7 and 8. The anode thickness thinning was lower than observed at the cathode, corresponding to a decrease of about 21% for cell 8.

Others microstructure changes in CLs were observed by SEM, cracks and delamination are some.

A very common feature among all of the analyzed CLs is the cracking. Figure 5 (a) shows a SEM image of a cracked CL. The integrity of the CL is compromised by cracks, but leaves the Nafion^{TM} membrane mechanically undamaged (fig. 5b). Thus, the fuel cell can still operate, but performance and durability may be reduced. On the other hand, the cracks will provide areas where the water could accumulate preventing reactant gases to reach the catalytic sites and consequently, reduces the reaction rate. Another important consequence is the catalyst erosion due to the exposure of the catalyst surfaces to agents such a water and gas flux.

In addition to cracks through the electrode thickness, delaminations between the electrode and the membrane are real failure modes (fig. 5b). Even small delaminations may affect the integrity and mechanical response of the MEA. Evidence of delamination was seen in both fresh and aged samples, which may put the question of the influence of the method of preparation. However, it was more predominant in aged samples.This type of defect may result from MEA manufacturing procedure but can also be induced by the degradation of the catalytic layer. It forces the current to flow away from delaminated zones, through neighboring regions in which heat is locally produced. As these neighboring zones are

also prone to water accumulation, they may degrade faster than other parts of the catalytic layers.

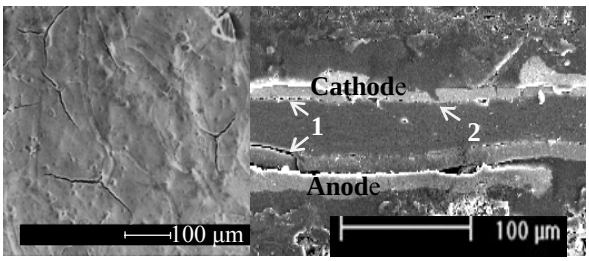

(a) (b)

Fig. 5 Scanning electron micrograph of a catalyst layer with cracks (anode cell 7) (a). Cross section SEM view of the MEA for cell 7 showing delamination (1) and cracking (2) (b).

The compression force and the uniformity of the compression force between the land and under the channel are further important factors to mitigate interfacial damage. The compression force distribution under the channel is dependent of diffusion media material properties, the land width, and assembly pressure. However, the compression force under the channel is significantly lower than that under the land and, consequently, the possible maximum size of interfacial delamination is likely to be the channel width.

Another type of catalyst layer degradation found was the presence of platinum clusters, which is evident in Figure 6. EDS analysis was performed on clustered areas, which were shown to be platinum rich. A spectrum of a surrounding area, where clusters were not observed, is included for comparison.

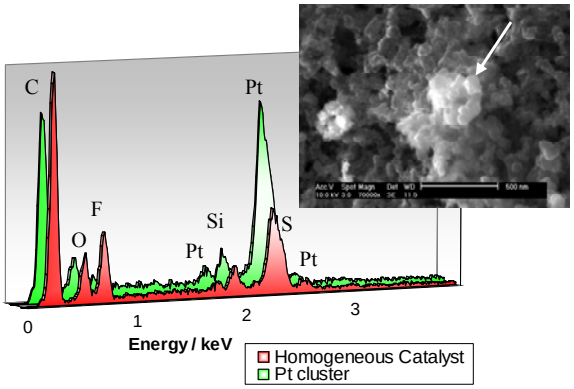

Fig. 6 Pt cluster on anodic layer C2, SEM and associated EDS on cluster and surrounding area.

The high platinum concentration could result from catalyst detaching from the carbon supporting surface. The catalyst agglomeration leads to a gradual decrease in the electrochemically active surface area, increasing in this way the activation loss. The presence Si has also been identified. The use of silicone piping and the sealing gasket are believed to have introduced Si contamination in the MEA.

From the EDS results it is suggested that a severe degradation occurred on the PTFE ionomer used as a binder in the catalytic layer, due the fluoride content loss.

3.2 Tunneling electron microscopy (TEM)

TEM supplies images of even higher magnification than the SEM, but it requires ultra thin sample specimen preparation. With a TEM study it was also possible to determine chemical identity, particle size and distribution and location of the lost catalyst in the investigated sample.

One of the more significant causes of fuel cell performance degradation is the catalyst deactivation during extended operation. TEM images were used to determine the electrocatalyst particle size and distribution on the carbon support in order to try to evaluate which mechanism is responsible for the performance loss.

For cell 2, migration of platinum particles is evident in Figure 7a). The Pt-enriched zone was higher at the cathode CL/Nafion interface, with an enrichment depth of about 100 nm. According with the EDS results for the anode and cathode areas, there is an increment in Pt content (wt%) for the interfaces (anode/membrane and cathode /membrane) of 55.5% and 84.3%, respectively.

Probably this occurred by the Ostewald ripening mechanism, which involves platinum dissolution at the cathode, diffusion of the soluble platinum species from small to large particles into the interface cathode/membrane, followed by redeposition of soluble Pt into large particles (fig.7b).

A random selection of 35 spherically shaped platinum particles in the TEM images, revealed a more frequent Pt particle diameter of 3.75 nm for all the selected areas at the anodic catalyst layer. For the cathodic layer, the Pt particle diameter more frequent increases from 2.94 nm to 3.53 nm, as the examined area extends towards the membrane. Aparently, the platinum particle shape was unchanged, suggesting that a few Pt particles dissolved and migrate to the interface where they agglomerate due to the thermodynamically instability of the nanoparticles.

Another feature observed by TEM was a presence of platinum inside the membrane of cell 4, at 2 mm from the anode (fig. 8 a), which probably results from carbon corrosion at the cathode. The loss of Pt from the carbon support and the loss of electrode

activity are the main responsible for the performance decrease.

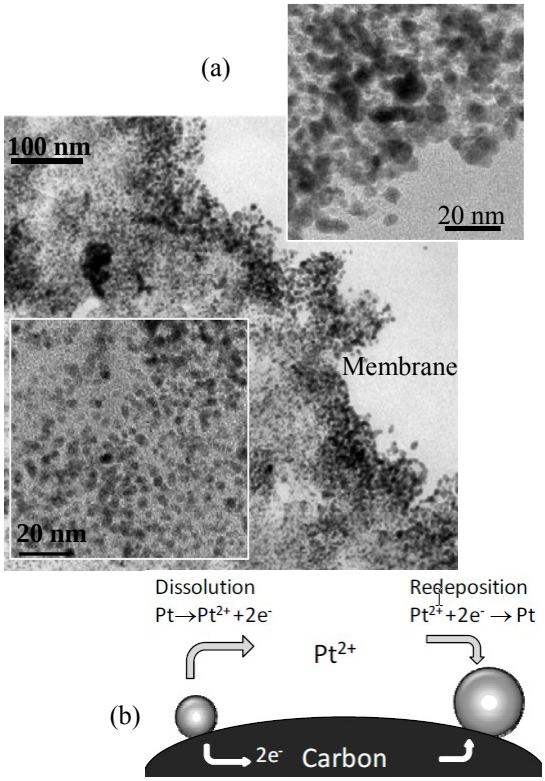

Fig. 7 TEM micrographs of cell 2 obtained from cathode (a) locations near the membrane interface. The mechanism probably responsible for the catalyst surface area loss (b).

Hydrogen molecules can permeate through the proton-conducting membrane leading to a chemical reduction of any dissolved Pt that migrate through the membrane, resulting in deposition. (fig. 8b) The location of this Pt deposition in the membrane is dependent on the partial pressure of oxygen in the cathode. The higher the partial pressure of oxygen, the farther from the cathode the Pt deposition occurs. The deposited platinum particle changed from the original shape (spherical) now showing a rectangular shape (fig. 8c) which, from the literature, is an indicative of this mechanism [16,17] .

Detachment of Pt nanoparticles from the carbon support and agglomeration of Pt nanoparticles is generally induced by carbon corrosion, so probably this had also happened on the stack. Corrosion on carbon support consists on its oxidation to form carbon dioxide. The corrosion rate depends, among other factors, on the type of carbon, operating potential, temperature, humidity, and uniformity of fuel distribution.

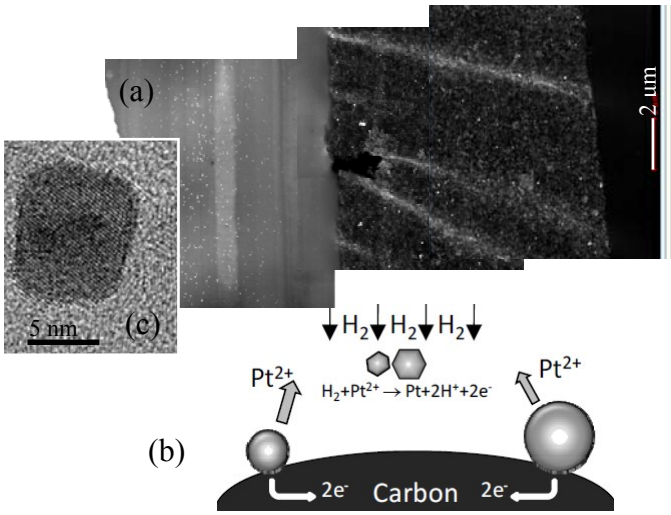

Fig. 8 TEM micrographs of cell 4 obtained from the anodic side where a platinum band it is visible in the membrane (a). A high magnification image of one of these particles found inside the membrane (c). The possible mechanism that occurred (b).

Carbon corrosion may occur:

- during the fuel operation at elevated temperatures [18] ;
- with start/stop operation (occuring on the cathode) [19] ;
- Fuel starvation (occurring on the anode) [20].

At anodic layer of cell 7, carbon particles are visible without any platinum particles, suggesting platinum dissolution and further migration and agglomeration inside the catalyst layer with larger sizes occurred (fig. 9). In this layer, void spaces and brighter areas are also observed indicating the possibility of carbon corrosion.

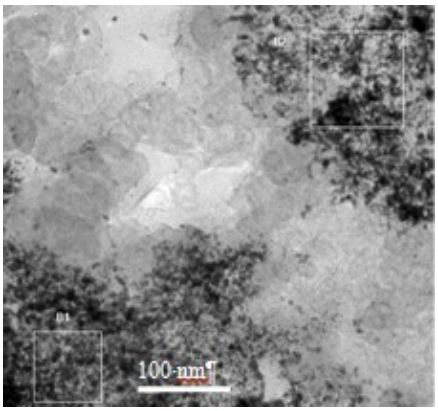

Fig. 9 TEM micrographs of cell 7 obtained from inner layer inside the anode.

Final remarks

Joint analysis of individual cells of a low power fuel cell stack using SEM, TEM and EDS was undertaking in order to identify main degradadtion mechanisms after 34 % loss in performance.
TEM allows direct imaging and evaluation of individual constituents (carbon support, ionomer, electrocatalyst particles, and interfaces between the electrode and membrane), while SEM allows the investigation of surfaces of the electrodes at higher magnifications which were useful for microstructural analysis.
Thickness variation was verified on both CLs. The cathode of all cells showed a thinning which is more pronounced as the cells were located farther from the hydrogen inlet in the stack. Cell 8 showed a thinning of about 47% after all the tests. At the anodic layer the thinning is meaningful only for cells 7 and 8.
The membrane thickness was unchanged.
EDS results indicated that severe degradation occurred on the PTFE ionomer used as a binder in the catalytic layer, due to fluoride content loss.
Changes in the CL surface were also observed, particularly particle coalescence and loss of porosity.
Carbon corrosion and catalytic active area loss mechanisms associated to platinum migration, or dissolution and re-deposition, were identified in a few samples. Further study is planned.

References

[1] B. C. H. Steele and A. Heinzel. Materials for fuel-cell technologies, *Nature* 414 (2001) 345–352.

[2] X. Cheng, L. Chen, C. Peng, Z. Chen, Y. Zhang and Q. Fan. Catalyst Microstructure Examination of PEMFC Membrane Electrode Assemblies *vs.* Time, *J. Electrochem. Soc*. 151 (2004) A48–A52.

[3] B. Avasarala, R. Moore and P. Haldar. Surface oxidation of carbon supports due to potential cycling under PEM fuel cell conditions, *Electrochimica Acta* 55(2010) 4765-4771.

[4] J.Wu, X. Z. Yuan, J. J. Martin, H. Wang, J. Zhang, J. Shen, S.Wu,W. Merida. A review of PEM fuel cell durability: Degradation mechanisms and mitigation strategies, J. Power Sources 184 (2008) 104–119.

[5] K. J.J. Mayrhofer, J. C. Meier, S. J. Ashton, G.K.H. Wiberg, F. Kraus, M. Hanzlik and M. Arenz. Fuel cell catalyst degradation on the nanoscale, *Electrochem. Commun.* 10 (2008) 1144–1147.

[6] W. Yoon and X. Huang. Study of Polymer Electrolyte Membrane Degradation under OCV Hold Using Bilayer MEAs, *J. Electrochem. Soc.* 157(2010) B599-B606.

[7] M.A. Rubio, A. Urquia and S. Dormido. Diagnosis of performance degradation phenomena in PEM fuel cells. Internat. J. .Hydrogen Energy 35 (2010) 2586-2590.

[8] P Rama, R Chen and J Andrews. A review of performance degradation and failure modes for hydrogen-fuelled polymer electrolyte fuel cells, J. Power and Energy 222 (2008) 421-441.

[9] W. Schmittinger, A. Vahidi. A review of the main parameters influencing long-term performance and durability of PEM fuel cells. *J Power Sources* 180 (2008) 1–14.

[10] S. Kundu, M.W. Fowler, L.C. Simon and S. Grot. Morphological features (defects) in fuel cell membrane electrode assemblies, *J. Power Sources* 157 **(**2006) 650–656.

[11] J. Xie, I.D.L. Wood, K.L. More, P. Atanassov and R.L. Borup. Microstructural Changes of Membrane Electrode Assemblies during PEFC Durability Testing at High Humidity Conditions, *J. Electrochem. Soc* **152** (2005). A1011–A1020.

[12] J. Xie, D.L. Wood, D.M. Wayne, T.A. Zawodzinski, P. Atanassov and R.L. Borup. Durability of PEFCs at High Humidity Conditions. *J. Electrochem. Soc.* **152** (2005) A104–A113.

[13] K.L. More, K.S. Reeves, J. Bentley and J. Xie, 2004, available from: http://www.hydrogen.energy.gov/pdfs/progress04/ivi2_more.pdf

[14] R.A. Silva, "Performance and Limitations in PEM Fuel Cells", Master Thesis (MPhil), University of Manchester, 2011.

[15] D.T. Santa Rosa, D.G. Pinto, V.S. Silva, R.A. Silva and C.M. Rangel. High Performance PEMFC Stack with Open-Cathode at Ambient Pressure and Temperature Conditions,. *Int. J. Hydrogen Energy* 32 (2007) 4350-4357.

[16] P.J. Ferreira, G.J. La, O.Y. Shao-Horn, D. Morgan, R. Makharia, S. Kocha, H.A. Gasteiger. Instability of Pt/C Electrocatalysts in Proton Exchange Membrane Fuel Cells: A mechanistic investigation, *J. Electrochem. Soc*. 152,(2005) A2256-2271.

[17] P. J. Ferreira, Y. Shao-Horn. Formation Mechanism of Pt Single-Crystal Nanoparticles in Proton Exchange Membrane Fuel Cells, *Electrochem. Solid-State Lett*. 10 (2007) B60-B63.

[18] L.M. Roen, C.H. Paik and T.D. Jarvi. Electrocatalytic corrosion of carbon support in PEMFC cathodes, *Electrochem. Solid-State Lett.* 7 (2004) A19–A24.

[19] Y. Ishigami, K. Takada, H. Yano, J. Inukai, M. Uchida, Y. Nagumo, T. Hyakutake, H. Nishide and M. Watanabe. Corrosion of Carbon Support at Cathode during H2/air Replacement at Anode Studied by Visualization of Oxygen Partial Pressure in a PEFC-Star-up/ Shut- down Simulations, *J. Power Sources* 196 (2011) 3003-3008.

[20] C.A. Reiser, L. Bregoli, T.W. Patterson, J.S. Yi, J.D. Yang, M.L. Perry and T.D. Jarvi. A reverse-current decay mechanism for fuel cells, *Electrochem. Solid-State Lett.* 8 (2005) A273–A276.